ACS OMEGA

http://pubs.acs.org/journal/acsodf

Article

MSW Compost Valorization by Pyrolysis: Influence of Composting Process Parameters

Alberto Palma,* Victor M. Doña-Grimaldi, Mercedes Ruiz-Montoya, Inmaculada Giráldez, Juan Carlos García, Javier Mauricio Loaiza, Francisco López, and Manuel J. Díaz

Cite This: *ACS Omega* 2020, 5, 20810−20816

Read Online

ACCESS | Metrics & More | Article Recommendations

ABSTRACT: The valorization of urban solid waste compost (MSW) in two different composting conditions (different aeration and humidity) has been studied (we work with the hypothesis that the composting process can have a significant influence on a subsequent pyrolysis process). The influence of composting on subsequent pyrolysis of the material was assessed by examining the kinetics of the process, maximizing hydrogen production and minimizing the activation energy. The thermogravimetric analysis carried out on the samples have shown that they have a greater loss of weight of 9−14% at 270−275 °C and 22−27% at 444−446 °C. Using the Kissinger−Akahira−Sunose method, the activation energy values are found to be in the range of 57.78−581.69 kJ mol^{-1}, and the assumption that pyrolysis of compost could be modeled by a first-order reaction may be a suitable approximation. The analysis of the gases produced from the pyrolysis process revealed that hydrogen increases in concentration as composting time advances until intermediate time. In this form, the composting process could be a suitable previous treatment for improving the pyrolysis process. In fact, decreasing aeration and moisture in the MSW composting process led to the production of an increased amount of hydrogen (8.3%) by pyrolysis of the resulting compost and also to a decreased activation energy (102.8 kJ mol^{-1}). These effects were also observed before the end of the composting process in the form of maximum hydrogen production and minimum activation energy after 20 days.

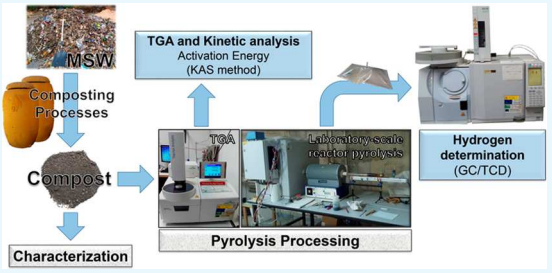

1. INTRODUCTION

Both population growth and increased economic development have led to an increase in global energy demand and environmental degradation. Also, climate change, related to the use of greenhouse gases from fossil fuels, has stimulated the production of energy from renewable sources instead of fossil fuels.[1] In this framework, solid urban waste (MSW) can be a satisfactory alternative, susceptible of being optimized, for obtaining energy. MSW combustion for the energy recovery has some well-known problems: high moisture that they possess and atmospheric contamination by heavy metals and products of incomplete combustion, dioxines, etc.[2] However, composting is considered one of the most sustainable methods of the recovery of MSW.[3] Compost is a stable final product that can be beneficially applied to land[4] and is suitable for managing large quantities of MSW in a sustainable way and for its recycling, but due to environmental problems with soil and overproduction, not all produced compost can be used as fertilizer.

As per European legislation, MSW and any compost obtained from it must be exploited or appropriately disposed of under Directive 2008/98/EC and European Environment Agency (2016).[5,6] This has required developing new ways of reclaiming compost. In this sense, various studies have demonstrated the viability of compost as an energy source.[7−9] The most obvious process for the energy use of compost could be the combustion process, but due to the high energy and environmental efficiency of pyrolysis, it is a cleaner process than combustion, reducing emissions of polluting gases and improving the quality of the residual ashes;[10] it has proven to be an effective method for converting biomass into synthesis gas (CO + H_2).[11] Pyrolysis is carried out in the absence of oxygen, decomposing the materials at temperatures of up to 800 °C and finally obtaining mainly gases CO, H_2, CH_4, and H_2O.[12] In addition, pyrolysis has another advantage over combustion and gasification that it has lower temperature requirements.

For the above reasons, pyrolysis is considered an effective method for obtaining bioenergy and reducing greenhouse gas emissions.[13] Also, in the pyrolysis process, a solid phase (biochar) could be obtained. Biochar is a valorizable product

Received: April 22, 2020
Accepted: June 29, 2020
Published: August 12, 2020

with uses in agriculture for improving carbon sequestration capacity and the physicochemical characteristics of soil.[14,15] At this point, optimizing the pyrolysis of MSW-derived compost and ensuring its viability entail examining the kinetics of the process and monitoring its activation energy.[16−18]

Decreased activation energy is known to increase the energy efficiency of a pyrolytic process. In fact, activation energy is the minimum amount of energy required for the molecular bonds involved in a reaction to be broken. As a result, low activation energy results in a faster, easier to start reaction.[19] As shown here, composting decreases the activation energy of the pyrolysis process.

It is not easy to identify the operating conditions that will decrease the activation energy of pyrolysis because the process initially involves the decomposition of the compounds with the weakest linear chains such as hemicelluloses, which require only 90−225 kJ mol^{-1}[20] of activation energy. The random cleavage of such linear chains increases the proportion of cellulose present in the material and hence the activation energy by 90−225 kJ mol^{-1} according to Ma et al.[21] and 145−285 kJ mol^{-1} according to Vamvuka et al.[22]

There are other unexplored, highly interesting ways of using pyrolysis gases including hydrogen production. In fact, some authors have obtained pyrolysis gases in proportions of 38−50% (v/v) from various other materials.[23,24]

Thermogravimetric analysis (TGA) has proved to be an effective choice for elucidating the kinetics of a pyrolysis process and determining its activation energy.[25,26] Specifically, when the TGA response (%W vs time) is measured at a number of different heating rates (greater or equal to three), kinetic parameters of activation energy (E_a) can be estimated by various methods.[27] According to White et al.[16] "understanding pyrolysis kinetics is vital to find out the feasibility, design and scaling for this technology". The different techniques used as model-fitting and model-free techniques, which include (or not) the identification of the reaction model, with small differences in the fit parameters of the models, allow us to estimate kinetic parameters, based on the data obtained from the TGA.[28] The use of model-free isoconversional methods may be appropriate for the estimation of kinetic parameters in pyrolysis because their use does not imply the need for a selected mechanism. Therefore, for each selected conversion, an independent activation energy can be calculated. These models, for compost, with multiple chemical compounds, for each conversion different compounds may be degrading and therefore different kinetic parameters can be calculated. To calculate the potential generated hydrogen quantities, a laboratory-scale reactor was used. In this study, the Kissinger−Akahira−Sunose (KAS) method is used. A great advantage of using this method is that the thermal degradation mechanism is not required.[29]

Also, the analysis of the gases emitted during the pyrolysis process is essential to know the impact of the process on the environment and its potential as a source of bioenergy.[13] To calculate the potential generated hydrogen quantities, a laboratory-scale reactor was used.

The aim of this work was to assess the effectiveness of composting municipal solid waste (MSW) for its subsequent valorization by pyrolysis. This entailed examining the influence of the composting variables on the activation energy of the pyrolysis process and the production of hydrogen as main valorizable gas.

2. RESULTS AND DISCUSSION

2.1. Composting Process. Two composting processes were conducted, as described in Section 4.1, both developing as expected. That is to say, the initial mesophilic phase (T < 40 °C) with an approximate duration of 2 days was followed by an increase in temperature giving rise to the thermophilic phase (T > 40 °C), with a duration of 5 days in both reactors, reaching maximum temperatures of 55 and 58 °C at 6 and 8 days of composting for reactors R1 and R2, respectively, and finally, a final or maturation phase was obtained, in which there was a slow decrease in temperature. Different temperature profiles in the composting process have been caused by the variation in composting conditions (data not shown). During the last phase of the composting process, the temperature profile was similar in both reactors. After 40 days of composting, the temperature of the reactors tended to equalize with the ambient temperature.

The significant characterization of MSW is shown in Table 1. As expected, due to the degradation of organic matter during composting, the organic matter content was reduced during the process in all mixtures.

Table 1. Significant Characteristics of MSW Samples Over the Dry Basis

property	MSW (raw material)	compost R1 (40 days later)	compost R2 (40 days later)
Kjeldahl-N (g kg^{-1})	22.1 (3.6)[a]	13.0 (10)	17.4 (8.6)
organic matter[b] (g kg^{-1})	702.0 (4.1)	598.0 (5.3)	573.0 (4.8)
EC (1:5 extract) (day s m^{-1})	8.3 (8.4)	10.2 (12.7)	11.1 (8.1)
pH (1:5 extract)	5.9 (3.4)	6.9 (1.4)	7.0 (1.4)
C/N ratio	19.1	24.3	20.0
particle size (%)			
<2 mm	2.7 (37)		
5−2 mm	4.9 (32.7)		
10−5 mm	9.9 (28.3)		
25−10 mm	27.3 (19.8)		
>25 mm	55.2 (16.1)		

[a]Average (% relative standard deviation). [b]MSW samples <5 mm and without impurities.

Significant differences in degradation have been found because process conditions affect the amount of organic matter degraded and the temperature profile. The values of biodegradability constant of 0.36 and 0.42 for R1 and R2 conditions, respectively, were calculated using the equation K_b = [(OMi − OMf) 100]/[OMi(100 − OMf)],[4] where OMf and OMi are the OM content at the end and at the beginning of the process, respectively.

In this way, higher biodegradability values have been observed under R2 composting conditions. Higher biodegradability means an improvement in organic matter mineralization, and therefore, there was a higher stability of the final components under R2 conditions.

Table 2 gives the elemental analysis of the compost samples. This composition was reported in a previous work.[30]

2.2. Pyrolysis Process of Compost. As noted earlier, pyrolyzing MSW-derived compost is thought to be a more energetically and environmentally efficient process than burning the compost. Also, it is expected to allow a stable material such as compost, which is difficult to market but must

https://dx.doi.org/10.1021/acsomega.0c01866
ACS Omega 2020, 5, 20810−20816

Table 2. Elemental Composition (%) of Compost in Reactors R1 and R2

reactor	compost	C	O	H	N
R1	day 1	29.4 (3.1)[a]	12.7 (3.9)	3.9 (5.1)	4.8 (6.3)
	day 10	26.4 (4.5)	13.3 (4.5)	2.4 (8.3)	3.9 (5.1)
	day 20	23.1 (4.8)	13.0 (4.6)	3.3 (6.1)	4.1 (4.9)
	day 40	19.0 (3.7)	12.6 (4.8)	3.1 (6.5)	4.2 (7.1)
R2	day 1	29.3 (3.8)	12.7 (4.7)	3.8 (5.3)	4.9 (4.1)
	day 10	26.1 (5.4)	11.3 (5.3)	2.8 (7.1)	4.6 (6.5)
	day 20	24.7 (4.9)	16.4 (4.9)	2.6 (7.7)	3.7 (5.4)
	day 40	21.5 (4.7)	13.8 (4.3)	3.5 (5.7)	4.0 (7.5)

[a]Average (% relative standard deviation).

be exploited or properly disposed of according to European laws, to be valorized.

The effect of the heating rate on the degradation of organic matter (TGA) as well as the differential mass loss thermograms (DTG) of the compost obtained in the reactors tested (R1 and R2) and in four different days of the composting process (days 1, 10, 20, and 40) at a heating rate of 15 °C min^{-1} has been studied (Figures 1 and 2). It is known that the organic fraction of compost, similar to biomass, is composed mainly of three organic components: cellulose, hemicellulose, and lignin (or derivatives).[4] According to the conclusions of Haug,[4] the mechanism of the pyrolysis process could be considered as an aggregate of the pyrolysis processes of these three main components.

As expected in biomass degradation, the four degradation regions in both thermograms (TGA and DTG) are observed. These regions are: (i) evaporation of water (45−200 °C), (ii) hemicellulosic fraction degradation (200−300 °C), (iii) cellulosic fraction degradation (300−400 °C), and (iv) ligninic fraction degradation (400−550 °C). The four regions have been found for the two reactors. For the studied compost, the first region between 80 and 160 °C associated with the evaporation of the adsorbed water in the samples is observed. Also, according to Yang et al.[9] it is known that both the size and the width of the peaks found during the thermal decomposition process depend on the composition and concentration of their main biomass components. In this study, it was found that the decomposition by pyrolysis of hemicellulose occurred between 200 and 300 °C, the decomposition of cellulose between 300 and 400 °C, and the decomposition of lignin in the wide range of 400−500 °C.

For the studied compost, two peaks between 200−300 and 300−400 °C, which may be related to the decomposition of hemicellulose and cellulose, can be observed. According to Van de Velden et al.[31] fluctuations above 600 °C occur may be due to lignin degradation, which can be very prolonged due to the high thermal stability of this compound. More specifically, in the TGA (15 °C min^{-1}), thermograms for R1 showed the maximum weight loss for 37.1, 31.6, 32.5, and 32.1% for days 1, 10, 20, and 40, respectively, and the maximum weight loss for 35.4, 32.1, 31.1, and 33.3% for days 1, 10, 20, and 40, respectively, for R2.

It should also be noted that, as the composting process advances, a lower intensity on the peaks corresponding to the degradation of organic matter (300−550 °C) is observed. This is due to the mineralization (and its corresponding losses on the different organic matter fractions) that occurred during the composting process. The inorganic constituents promote secondary reactions that cause the breakdown of higher molecular compounds to smaller ones.[32] In this way, according to Rakthong et al.[33] composting may increase the stability, degree of aromatization, and molecular weight of non-mineralized organic components, so these changes may explain the lower intensity of the peaks found in the figures. On the other hand, no significant difference either in temperature peaks or in maximum weight loss rate has been found between processes with different reaction conditions (R1 and R2). Although the increased degree of biodegradation obtained under the set R2 of operating conditions (i.e., with the highest aeration and moisture values) can be associated with the increased stability of the end product (compost), the conditions of the set R1 led to higher energy efficiency in the subsequent pyrolysis process. Also, because composting costs are largely dictated by aeration,[34] R1 is more economical than R2.

2.3. Kinetic Analysis of the Pyrolysis Process. The evolution of E_a, calculated according to eq 4, for the process conditions studied and according to the composting time (days 1, 10, 20, and 40) and its coefficients of determination (R^2) are shown in Table 3. For example, KAS equations ($\ln(\beta/T^2)$ vs $(1/T)$) at a heating rate of 15 °C min^{-1} are also shown in this table.

In this table, regression results in R^2 were adequate in the range of 0.93−0.99. In this way, although a high R2 is a necessary but not a sufficient condition for the assumption that the weight loss can be described by a single activation energy at a particular conversion, the hypothesis that pyrolysis of compost could be modeled under a first-order reaction could be properly established. Obviously, different activation energies can be observed among the studied conversions. This may be due to the successive breakdown and volatilization of compost components of different reactivities, as suggested by Figures 1

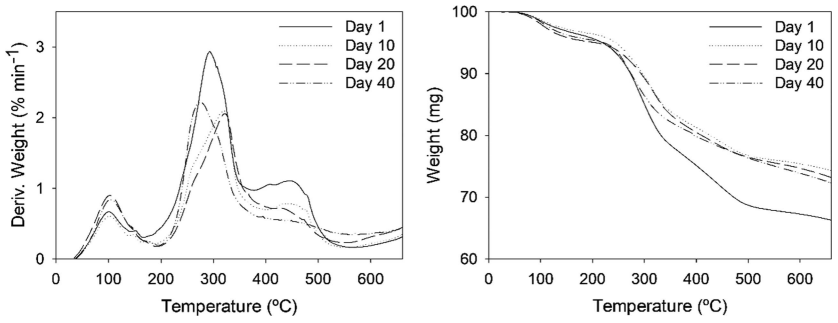

Figure 1. Experimental TGA and DTG curves of the pyrolysis process of the samples collected from the composting process (reactor 1: 0.050 L kg^{-1} day^{-1} aeration and 40% moisture) at different times.

https://dx.doi.org/10.1021/acsomega.0c01866
ACS Omega 2020, 5, 20810−20816

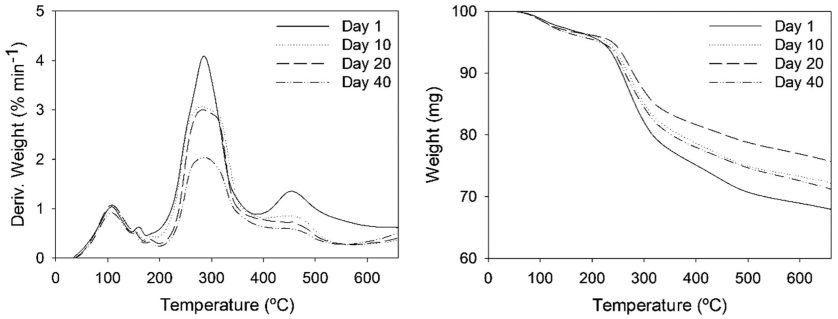

Figure 2. Experimental TGA and DTG curves of the pyrolysis process of the samples collected from the composting process (reactor 2: 0.175 L kg^{-1} day^{-1} aeration and 55% moisture) at different times.

Table 3. Evolution of Activation Energy According to Composting Time and Conditions (R1 and R2) for Conversion Degrees of α = 0.20 and 0.90, Respectively, in the Pyrolysis Process

		α = 0.20				α = 0.90			
	compost	slope	*y*-intercept	R^2	E_a (kJ mol^{-1})	slope	*y*-intercept	R^2	E_a (kJ mol^{-1})
R1	day 1	−9.89	1.84	0.94	225.73	−11.09	1.01	0.94	581.69
	day 10	−9.93	1.81	0.96	300.55	−11.12	0.99	0.96	425.90
	day 20	−9.95	1.78	0.97	57.78	−11.12	0.99	0.97	102.83
	day 40	−9.88	1.85	0.97	92.95	−11.15	0.98	0.98	202.48
R2	day 1	−9.82	1.91	0.94	201.20	−11.11	0.99	0.94	251.09
	day 10	−9.84	1.88	0.93	131.34	−11.12	0.99	0.93	186.12
	day 20	−9.86	1.86	0.95	82.37	−11.13	0.99	0.95	146.59
	day 40	−9.84	1.89	0.94	86.66	−11.12	0.99	0.94	166.99

and 2. At low conversion, the more reactive components were volatilized, but as pyrolysis proceeded, only the most resistant components were left to be broken down and volatilized so that the activation energy was higher at 90% than at 20% conversion. Activation energy depended to a greater extent on the number of days of composting, probably because the progress of the composting process changed the strength of the molecular structure.[35]

At the beginning of the composting process, a higher E_a value is obtained in the first-step reaction (α = 0.20). It can be due to the high hemicellulose content in the compost. According to Rueda-Ordóñez and Tannous,[36] hemicellulose activation energy is lower than that calculated for celluloses. In this manner, in both reactors, E_a values in the compost at the end of the process (day 40) have been lower than those at the beginning (day 1). This may be due to the higher cellulose content at the beginning of the composting process than that found after 40 days of composting. As mentioned above, activation energy depended to a greater extent on the number of days of composting, but cellulose component degradation could mark the value of its activation energy.[37] On the other hand, the relative ash content of the resulting biochars increased with the course of the composting process. The increase in ash content is the result of mineral concentration and destructive mineralization of lignocellulosic matters as the composting process progresses. The E_a values found at α = 0.9 are usually higher than those at α = 0.20 because initially the organic matter is more easily degraded. As the pyrolysis reaction advances, progressively, the more recalcitrant compounds with higher E_a values are decomposed.

After only 20 days, which shortens the usual composting times, a product that can be used for suitable pyrolysis can be obtained because the activation energy for pyrolysis as calculated from the TGA results has decreased to a low figure.

2.4. Hydrogen Obtained During Pyrolysis. As stated above, pyrolysis allows MSW compost to be valorized with potential economic advantages over on-site burning of the waste for energy production. In fact, pyrolysis avoids the loss of energy through "heating" of the excess surrounding air during burning and provides hydrogen as the main valorizable gas. We assessed hydrogen production from MSW composted under two different sets of conditions (R1 and R2). The aim was not only to boost hydrogen production by pyrolysis but also to decrease the activation energy of the process to increase its energy efficiency. Figure 3 shows the variation of hydrogen production with the pyrolysis activation energy. The activation energy at α = 0.9 was selected because this corresponded to almost full conversion and hence to the maximum gas yield, which is what would be obtained under the laboratory-scale reactor conditions. In this sense, H_2 concentration evolution in

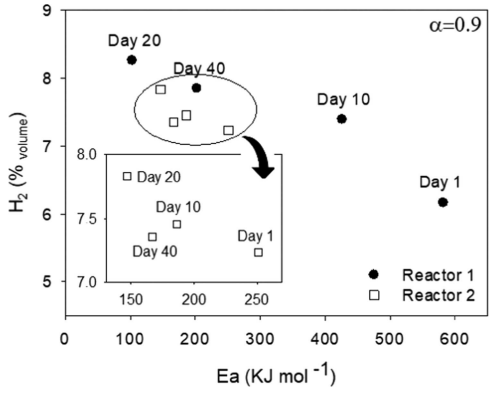

Figure 3. Relationship between the H_2 produced (% volume) and E_a obtained (for α = 0.90) in the pyrolysis process of the compost studied for both reactors.

https://dx.doi.org/10.1021/acsomega.0c01866
ACS Omega 2020, 5, 20810−20816

the gas obtained under both composting processes for medium (day 20) and high (day 40) composting time with respect to initial composting time is found and, in fact, represents a significant increase. At the beginning of the composting process, hemicellulosic compounds are degraded. This causes a relative increase in cellulose and lignin concentrations. It is known[38] that these compounds have the main responsibility in hydrogen generation during pyrolysis.

In Figure 3, in general, a negative relationship between the concentration of H_2 and E_a can be noted with an exception for the 40 day compost. It is an important conclusion of our work that the suitable characteristics of a raw material, to be susceptible to pyrolysis, could be obtained with the minimum activation energy required for pyrolysis and high H_2 values in the resulting gas when the composting process was carried out at low aeration and moisture conditions and 20 days (intermediate) of the full process. According to conditions in Section 2.1, it is the case for the compost from R1 at day 20 with the highest amount of obtained hydrogen (8.3%), and on the other hand, for the compost from R1 at day 1 with the lowest amount of obtained hydrogen (6.2%). The obtained H_2 concentrations are similar to the obtained values in another study by biomass pyrolysis.[38] In addition, the maximum values for hydrogen concentrations found in both experiments for the minimum activation energy correspond, in all cases, to samples obtained at medium values of processing time.

3. CONCLUSIONS

The development of the MSW pyrolysis process is strongly dependent on the conditions of the previous composting process.

While an aeration rate of 0.175 L kg^{-1} day^{-1} and 55% moisture led to increased biodegradability, energy efficiency and hydrogen production in the pyrolysis process were substantially greater under milder composting conditions (viz., 0.050 L kg^{-1} $day^{-1}$and 40%).

TGA curves showed the four typical pyrolysis zones and revealed similar peaks of decomposition under both composting process conditions. No significant differences were found between the composting conditions. However, the analysis of the gases produced from the pyrolysis process revealed that hydrogen increases in concentration as composting time advances until intermediate time. In this form, to improve pyrolysis conditions, composting could be applied as an appropriate pretreatment process. In fact, decreasing aeration and moisture in the MSW composting process led to the production of an increased amount of hydrogen (8.3%) by pyrolysis of the resulting compost and also to a decreased activation energy (102.8 kJ mol^{-1}). These effects were also observed before the end of the composting process as maximum hydrogen production and minimum activation energy after 20 days.

4. MATERIALS AND METHODS

4.1. Municipal Solid Waste Used and the Composting Process. The raw material (MSW) was obtained from Villarrasa's urban waste treatment plant (Huelva-southern Spain). Two composting processes (with different aeration and moisture content) were studied in composting reactors of 200 liters. Polyurethane foam (to avoid heat loss) to cover the outside of the reactor was used. The two processes were, namely, R1 (aeration in L kg^{-1} day^{-1} = 0.050 ± 0.003 and moisture (%) = 40 ± 2) and R2 (aeration in L kg^{-1} day^{-1} = 0.175 ± 0.009 and moisture (%) = 55 ± 3). Aeration was added by compressed air and dispersed through a perforated plate at the bottom of the reactor. During the different phases of composting, water losses were measured and compensated daily to maintain the initial design conditions during the experiment. Tests in reactors were carried out in duplicate. The reactors were filled to their half (40 kg MSW) to ensure suitable headspace. Samples (100 g) were taken at different locations and at different depths in the reactors.

4.2. Characterization Methods. Samples (MSW) were sieved and residues such as plastics, metals, stones, and glass were separated (manually) and weighed. Moisture was determined by drying at 105 °C to constant weight. Organic matter and nitrogen were determined in the <5 mm size fraction. Before and after the pyrolytic process, the total organic matter (OM) was calculated by loss on ignition (550 °C for 5 h)[39] and carbon was estimated as OM/1.8.[4] Nitrogen (Kjeldahl-N) was determined by steam distillation after Kjeldahl digestion.[40] The pH and electric conductivity (EC) were determined in a 1/5 (in weight) compost/water extract using the pH and EC electrodes, respectively. Elemental composition was determined according to Milne et al.[41]

4.3. Laboratory-Scale Reactor Pyrolysis Processing of Samples. To calculate the potential generated hydrogen quantities, a laboratory-scale reactor was used. This reactor consisted of a quartz tube (10 mm diameter and 140 cm length) in a temperature-controlled furnace. The sample (approximately 1 g) was introduced by means of a horizontal actuator. The residence time was fixed at 7 min, the temperature at 700 °C, and nitrogen (250 cm^3 min^{-1}) was used as a transport gas.

The permanent gases were collected in 1 L Tedlar bags (Supelco, Bellefonte, PA), which were placed at the end of the process line. The gases were then analyzed offline using a gas chromatography−thermal conductivity detector (GC−TCD 2010, Shimadzu Corporation, Tokyo, Japan) equipped with a Carboplot P7 column (25 m long, 0.53 mm internal diameter, and 0.25 μm film thickness) (Agilent Technologies, Palo Alto, CA). The GC was equipped with a gas sampling valve (GSV) module as an injection port with a loop of 1 mL. The maximum of hydrogen was found between 3 and 5 min of the process. Hydrogen quantitative analysis was carried out by means of the external standard method by the mixture containing permanent gas standards (4% O_2, 20% H_2, 20% CO, 20% CO_2, and 10% CH_4 in He), which was supplied by Abelló Linde S.A. (Barcelona, Spain). Response factors were obtained for each of the standards in a five-point calibration curve and compared to the response factors from the samples.

4.4. TGA and Kinetic Modeling. The equipment used to determine pyrolysis parameters was a Mettler Toledo TGA/DSC1 STARe system model thermogravimetric analyzer. TGA conditions were N_2 flow rate of 15 cm^3 min^{-1} and heating rates of 5, 10, 15, and 20 °C min^{-1}, from 25 to 700 °C.

For the activation energy calculation, the Kissinger−Akahira−Sunose (KAS) method was used. In its mathematical expression, the KAS method is derived from eq 1. This equation is integrated from the initial condition of $\alpha = 0$ at $T = T_0$ and eq 2 is obtained.[42,43]

$$\left(\frac{d\alpha}{dT}\right) = \frac{A}{\beta}\exp\left(\frac{-E_a}{RT}\right) f(\alpha) \quad (1)$$

https://dx.doi.org/10.1021/acsomega.0c01866
ACS Omega 2020, 5, 20810−20816

$$G(\alpha) = \int_0^{\alpha} \frac{d\alpha}{f(\alpha)} = \frac{A}{\beta}\int_{T_0}^{T} \exp\left(\frac{-E_a}{R\,T}\right)dT \quad (2)$$

where α is the degree of the conversion in the process, β is the heating rate, $f(\alpha)$ is the reaction mechanism model, T is the temperature, R is the gas constant, and E_a is the activation energy.

After that, the Coats−Redfern approximation,[44] as displayed in eq 3, was used.

$$G(\alpha) = \frac{A}{\beta}\frac{RT^2}{E_a}\exp\left(\frac{-E_a}{RT}\right) \quad (3)$$

Taking the natural logarithm of eqs 3 and 4 is obtained.

$$\ln\left(\frac{\beta}{T^2}\right) = \ln\left(\frac{AR}{E_a G(\alpha)}\right) - \frac{E_a}{RT} \quad (4)$$

With the weight loss curves with respect to the thermal degradation temperature obtained after the tests with different heating curves and after the application of eq 4, a slope (E_a/R) from which it is possible to obtain the activation energy, for each type of composting and process time, could be obtained. The conversion degrees, for E_a estimations, can be selected in the differential mass loss thermograms (the maximums).

The NETZSCH Kinetics Neo (2.4.4.6) software was used to calculate the energies for both the raw material and the obtained products.

AUTHOR INFORMATION

Corresponding Author

Alberto Palma − *Research Center in Technology of Products and Chemical Processes, PRO2TECS-Chemical Engineering Department, Campus "El Carmen", University of Huelva, 21004 Huelva, Spain;* orcid.org/0000-0003-0420-1785; Email: alberto.palma@diq.uhu.es

Authors

Victor M. Doña-Grimaldi − *Research Center in Technology of Products and Chemical Processes, PRO2TECS-Chemical Engineering Department, Campus "El Carmen", University of Huelva, 21004 Huelva, Spain*

Mercedes Ruiz-Montoya − *Research Center in Technology of Products and Chemical Processes, PRO2TECS-Chemical Engineering Department, Campus "El Carmen", University of Huelva, 21004 Huelva, Spain*

Inmaculada Giráldez − *Department of Chemistry "Prof. J.C. Vílchez-Martín", Campus "El Carmen", University of Huelva, 21004 Huelva, Spain*

Juan Carlos García − *Research Center in Technology of Products and Chemical Processes, PRO2TECS-Chemical Engineering Department, Campus "El Carmen", University of Huelva, 21004 Huelva, Spain*

Javier Mauricio Loaiza − *Research Center in Technology of Products and Chemical Processes, PRO2TECS-Chemical Engineering Department, Campus "El Carmen", University of Huelva, 21004 Huelva, Spain*

Francisco López − *Research Center in Technology of Products and Chemical Processes, PRO2TECS-Chemical Engineering Department, Campus "El Carmen", University of Huelva, 21004 Huelva, Spain*

Manuel J. Díaz − *Research Center in Technology of Products and Chemical Processes, PRO2TECS-Chemical Engineering Department, Campus "El Carmen", University of Huelva, 21004 Huelva, Spain*

Complete contact information is available at: https://pubs.acs.org/10.1021/acsomega.0c01866

Notes

The authors declare no competing financial interest.

ACKNOWLEDGMENTS

This investigation received financial support from the Ministry of Economy and Competitiveness (Spain), the Regional Ministry of Innovation, Science and Enterprise, the Government of the Junta de Andalucía, Spain (project number RNM 2323-2012 and postdoctoral fellowship), and the National Program for Research Aimed at the Challenges of Society, CTQ2017-85251-C2-1-R.

REFERENCES

(1) Akubo, K.; Nahil, M. A.; Williams, P. T. Pyrolysis-Catalytic Steam Reforming of Agricultural Biomass Wastes and Biomass Components for Production of Hydrogen/Syngas. *J. Energy Inst.* **2019**, *92*, 1987−1996.

(2) McKay, G. Dioxin Characterisation, Formation and Minimisation during Municipal Solid Waste (MSW) Incineration: Review. *Chem. Eng. J.* **2002**, *86*, 343−368.

(3) Cabeza, I. O.; López, R.; Giraldez, I.; Stuetz, R. M.; Díaz, M. J. Biofiltration of α-Pinene Vapours Using Municipal Solid Waste (MSW) - Pruning Residues (P) Composts as Packing Materials. *Chem. Eng. J.* **2013**, *233*, 149−158.

(4) Haug, R. T. *The Practical Handbook of Compost Engineering*, 1st ed.; CRC Press, 1993.

(5) European Parliament, C. of the E. U., *Directive 2008/98/EC of the European Parliament and of the Council of 19 November 2008 on Waste and Repealing Certain Directives (Text with EEA Relevance)*, 2008.

(6) EEA, *More from Less - Material Resource Efficiency in Europe. 2015 Overview of Policies, Instruments and Targets in 31 Countries*, 2016.

(7) Ahmad, A. A.; Zawawi, N. A.; Kasim, F. H.; Inayat, A.; Khasri, A. Assessing the Gasification Performance of Biomass: A Review on Biomass Gasification Process Conditions, Optimization and Economic Evaluation. *Renewable Sustainable Energy Rev.* **2016**, *53*, 1333−1347.

(8) Dong, L.; Wu, C.; Ling, H.; Shi, J.; Williams, P. T.; Huang, J. Promoting Hydrogen Production and Minimizing Catalyst Deactivation from the Pyrolysis-Catalytic Steam Reforming of Biomass on Nanosized NiZnAlOx Catalysts. *Fuel* **2017**, *188*, 610−620.

(9) Yang, H. Characteristics of Hemicellulose Cellulose and Lignin Pyrolysis. *Fuel* **2007**, *86*, 1781−1788.

(10) Chen, S.; Meng, A.; Long, Y.; Zhou, H.; Li, Q.; Zhang, Y. TGA Pyrolysis and Gasification of Combustible Municipal Solid Waste. *J. Energy Inst.* **2015**, *88*, 332−343.

(11) Yang, S.; Zhang, X.; Chen, L.; Sun, L.; Zhao, B.; Si, H.; Xie, X.; Meng, F. Pyrolysis of Sawdust with Various Fe-Based Catalysts: Influence of Support Identity on Hydrogen Production. *J. Anal. Appl. Pyrolysis* **2019**, *137*, 29−36.

(12) Loaiza, J. M.; López, F.; García, M. T.; García, J. C.; Díaz, M. J. Integral Valorization of Tagasaste (Chamaecytisus Proliferus) under Thermochemical Processes. *Biomass Convers. Biorefin.* **2018**, *8*, 265−274.

(13) Domínguez, M. T.; Madejón, P.; Madejón, E.; Diaz, M. J. Novel Energy Crops for Mediterranean Contaminated Lands: Valorization of Dittrichia Viscosa and Silybum Marianum Biomass by Pyrolysis. *Chemosphere* **2017**, *186*, 968−976.

(14) Campos, P.; Miller, A. Z.; Knicker, H.; Costa-Pereira, M. F.; Merino, A.; De la Rosa, J. M. Chemical, Physical and Morphological Properties of Biochars Produced from Agricultural Residues:

Implications for Their Use as Soil Amendment. *Waste Manage.* **2020**, *105*, 256−267.
(15) Yadav, V.; Khare, P. Impact of Pyrolysis Techniques on Biochar Characteristics: Application to Soil. In *Biochar Applications in Agriculture and Environment Management*; Springer International Publishing, 2020; pp 33−52.
(16) White, J. E.; Catallo, W. J.; Legendre, B. L. Biomass Pyrolysis Kinetics: A Comparative Critical Review with Relevant Agricultural Residue Case Studies. *J. Anal. Appl. Pyrolysis* **2011**, *91*, 1−33.
(17) Lin, Y. C.; Cho, J.; Tompsett, G. A.; Westmoreland, P. R.; Huber, G. W. Kinetics and Mechanism of Cellulose Pyrolysis. *J. Phys. Chem. C* **2009**, *113*, 20097−20107.
(18) Bhagavatula, A.; Huffman, G.; Shah, N.; Honaker, R. Evaluation of Thermal Evolution Profiles and Estimation of Kinetic Parameters for Pyrolysis of Coal/Corn Stover Blends Using Thermogravimetric Analysis. *J. Fuels* **2014**, *2014*, 1−12.
(19) Amini, E.; Safdari, M. S.; Weise, D. R.; Fletcher, T. H. Pyrolysis Kinetics of Live and Dead Wildland Vegetation from the Southern United States. *J. Anal. Appl. Pyrolysis* **2019**, *142*, No. 104613.
(20) Aburto, J.; Moran, M.; Galano, A.; Torres-García, E. Non-Isothermal Pyrolysis of Pectin: A Thermochemical and Kinetic Approach. *J. Anal. Appl. Pyrolysis* **2015**, *112*, 94−104.
(21) Ma, Z.; Chen, D.; Gu, J.; Bao, B.; Zhang, Q. Determination of Pyrolysis Characteristics and Kinetics of Palm Kernel Shell Using TGA-FTIR and Model-Free Integral Methods. *Energy Convers. Manage.* **2015**, *89*, 251−259.
(22) Vamvuka, D.; Kakaras, E.; Kastanaki, E.; Grammelis, P. Pyrolysis Characteristics and Kinetics of Biomass Residuals Mixtures with Lignite. *Fuel* **2003**, *82*, 1949−1960.
(23) Olaleye, A. K.; Adedayo, K. J.; Wu, C.; Nahil, M. A.; Wang, M.; Williams, P. T. Experimental Study, Dynamic Modelling, Validation and Analysis of Hydrogen Production from Biomass Pyrolysis/Gasification of Biomass in a Two-Stage Fixed Bed Reaction System. *Fuel* **2014**, *137*, 364−374.
(24) Chen, F.; Wu, C.; Dong, L.; Vassallo, A.; Williams, P. T.; Huang, J. Characteristics and Catalytic Properties of Ni/CaAlOx Catalyst for Hydrogen-Enriched Syngas Production from Pyrolysis-Steam Reforming of Biomass Sawdust. *Appl. Catal., B* **2016**, *183*, 168−175.
(25) Mishra, R. K.; Mohanty, K. Pyrolysis Kinetics and Thermal Behavior of Waste Sawdust Biomass Using Thermogravimetric Analysis. *Bioresour. Technol.* **2018**, *251*, 63−74.
(26) Rasool, T.; Kumar, S. Kinetic and Thermodynamic Evaluation of Pyrolysis of Plant Biomass Using TGA. In *Materials Today: Proceedings*; Elsevier Ltd, 2020; Vol. *21*, pp 2087−2095.
(27) Hashimoto, K.; Hasegawa, I.; Hayashi, J.; Mae, K. Correlations of Kinetic Parameters in Biomass Pyrolysis with Solid Residue Yield and Lignin Content. *Fuel* **2011**, *90*, 104−112.
(28) Radojevic, M.; Balac, M.; Jovanovic, V.; Stojiljkovic, D.; Manic, N. Thermogravimetric Kinetic Study of Solid Recovered Fuels Pyrolysis. *Hem. Ind.* **2018**, *72*, 99−106.
(29) Starink, M. J. The Determination of Activation Energy from Linear Heating Rate Experiments: A Comparison of the Accuracy of Isoconversion Methods. *Thermochim. Acta* **2003**, *404*, 163−176.
(30) Doña-Grimaldi, V. M.; Palma, A.; Ruiz-Montoya, M.; Morales, E.; Díaz, M. J. Energetic Valorization of MSW Compost Valorization by Selecting the Maturity Conditions. *J. Environ. Manage.* **2019**, *238*, 153−158.
(31) Van de Velden, M.; Baeyens, J.; Brems, A.; Janssens, B.; Dewil, R. Fundamentals, Kinetics and Endothermicity of the Biomass Pyrolysis Reaction. *Renew. Energy* **2010**, *35*, 232−242.
(32) Bradbury, A. G. W.; Sakai, Y.; Shafizadeh, F. A Kinetic Model for Pyrolysis of Cellulose. *J. Appl. Polym. Sci.* **1979**, *23*, 3271−3280.
(33) Rukthong, W.; Thanatawee, P.; Sunphorka, S.; Piumsomboon, P.; Chalermsinsuwan, B. Computation of Biomass Combustion Characteristic and Kinetic Parameters by Using Thermogravimetric Analysis. *Eng. J.* **2015**, *19*, 41−57.
(34) Stentiford, E. I. Composting Control: Principles and Practice. In *The Science of Composting*; Springer: Netherlands, 1996; pp 49−59.
(35) Barneto, A. G.; Carmona, J. A.; Conesa Ferrer, J. A.; Díaz Blanco, M. J. Kinetic Study on the Thermal Degradation of a Biomass and Its Compost: Composting Effect on Hydrogen Production. *Fuel* **2010**, *89*, 462−473.
(36) Rueda-Ordóñez, Y. J.; Tannous, K. Isoconversional Kinetic Study of the Thermal Decomposition of Sugarcane Straw for Thermal Conversion Processes. *Bioresour. Technol.* **2018**, *196*, 136−144.
(37) Basu, P. *Biomass Gasification, Pyrolysis and Torrefaction*, 2nd ed.; Academic Press, 2013.
(38) Loaiza, J. M.; López, F.; García, M. T.; García, J. C.; Díaz, M. J. Biomass Valorization by Using a Sequence of Acid Hydrolysis and Pyrolysis Processes. Application to Leucaena Leucocephala. *Fuel* **2017**, *203*, 393−402.
(39) Klute, A.; Weaver, R. W.; Sparks, D. L.; Dane, J. H.; Topp, G. C. *Methods of Soil Analysis*; SSSA Book Series, 1986.
(40) Faithfull, N. T. *Methods in Agricultural Chemical Analysis A Practical Handbook*; Cabi, 2002.
(41) Milne, T. A.; Brennan, A. H.; Glenn, B. H. Solar Technical Information Program (U.S.). In *Sourcebook of Methods of Analysis for Biomass and Biomass Conversion Processes*; Elsevier Applied Science, 1990.
(42) Lim, A. C. R.; Chin, B. L. F.; Jawad, Z. A.; Hii, K. L. Kinetic Analysis of Rice Husk Pyrolysis Using Kissinger-Akahira-Sunose (KAS) Method. *Procedia Eng.* **2016**, *148*, 1247−1251.
(43) Li, H.; Niu, S.; Lu, C. Thermal Characteristics and Kinetic Calculation of Castor Oil Pyrolysis. In *Procedia Engineering*; Elsevier Ltd, 2017; Vol. *205*, pp 3711−3716.
(44) Coats, A. W.; Redfern, J. Kinetic Parameters from Thermogravimetric Data. *Nature* **1964**, *201*, 68−69.

https://dx.doi.org/10.1021/acsomega.0c01866
ACS Omega 2020, 5, 20810−20816